Flame retardancy of PET foams manufactured from bottle waste

Katalin Bocz[1] · Ferenc Ronkay[2,3] · Dániel Vadas[1] · Béla Molnár[2] · Dániel Gere[2,3] · Tibor Czigány[3,4] · György Marosi[1]

Abstract

Supercritical CO_2-assisted extrusion technique was used to produce flame retarded foams from recycled poly(ethylene terephthalate) (rPET). Synergistic combination of aluminium-alkylphosphinate flame retardant (FR) and natural montmorillonite (MMT) was utilised to provide adequate flame retardancy at moderate loadings, i.e. with less than 9% of additives. Addition of FR was found to increase the rate of degradation during production (compounding and foam extrusion), which was effectively compensated by chain extender (CE) addition that ensured the melt strength required to obtain proper foam structure. The effects of the FR content and the CE addition on the viscosity of the rPET compounds and on the morphological, thermal, flammability and mechanical properties of the foam products were comprehensively investigated. When compared to injection moulded bulk materials of identical compositions, the highly porous structure of foams was found to increase flammability according to UL94 tests and LOI measurements but has not been shown to be detrimental to heat release rates as measured by cone calorimetry. It was concluded that with well-balanced composition, i.e. 8% FR + 1% MMT + 1% CE, low-density foams (with porosities higher than 70%) of uniform microcellular structure and prominent flame retardant characteristics (such as V0 rating according to UL94 standard, LOI of 28.5% and by 50% reduced peak of heat release rate and by 30% reduced total heat emission) can be manufactured even from rPET.

Keywords Recycled PET · Extrusion foaming · Flame retardancy · Chain extender

Introduction

Plastics are generally petroleum-based and therefore easily flammable materials that is of serious concern for human health and safety. An estimated 370,000 residential building fires per year were reported to fire departments within the USA between 2017 and 2019. The fires caused an estimated 3,000 deaths, 12,000 injuries and $ 8 billion in property loss [1]. During this period, the number of fire-related deaths in the European Union is around 4,400, and the number of injuries is approx. ten times higher [2]. Polymeric insulation materials for household appliances and buildings pose a particular risk, as they allow a significantly shorter escape time due to their high heat of combustion, burning rate and toxic gases produced in the event of fires [3, 4]. For this reason, flame retardancy of plastic insulation is an increasingly important requirement. However, developments must also take into account the protection of the environment and human health, both in terms of the polymer used and the flame retardant additives used [5].

The packaging industry is primarily responsible for the large amounts of plastic waste generated [6]. The used short-lived polyolefin, polystyrene and poly(ethylene terephthalate) (PET) products generally become waste within one year of production [7, 8]. The selective collection and utilisation of these is now a clearly recognised task [9–11]. During recycling, a good solution can be to develop raw materials from which durable products can be produced that can be used for up to 15–20 years, e.g. construction or automotive foam insulations [12]. For these applications, the required

✉ Katalin Bocz
bocz.katalin@vbk.bme.hu

1. Department of Organic Chemistry and Technology, Faculty of Chemical Technology and Biotechnology, Budapest University of Technology and Economics, Műegyetem rkp. 3., 1111 Budapest, Hungary

2. Material Testing Laboratory, Imsys Ltd, Mozaik Street 14/A., 1033 Budapest, Hungary

3. Department of Polymer Engineering, Faculty of Mechanical Engineering, Budapest University of Technology and Economics, Műegyetem rkp. 3., 1111 Budapest, Hungary

4. MTA-BME Research Group for Composite Science and Technology, Muegyetem rkp. 3., 1111 Budapest, Hungary

flame retardant properties must be addressed in an environmentally friendly, halogen-free and cost-effective manner [13].

Metal phosphinates play a major role in the flame retardancy of polyesters, mainly due to their relatively high phosphorus content, good thermal stability and low affinity to moisture [14]. The fire retardancy mechanism of a metal phosphinate salt (aluminium diethylphosphinate (AlPi)) in a polyester was firstly analysed by *Schartel* and *Braun* [15]. They found that in poly(butylene terephthalate) (PBT), AlPi has strong gas-phase activity, as it decomposes by releasing diethylphosphinic acid which acts as effective flame inhibitor. Besides, aluminium-terephthalic salt formation was also evinced in the condensed phase, creating slightly increased amount of char. In cone calorimeter tests, however, the carbonaceous layer which forms in the presence of inorganic components (mainly aluminium phoshates) showed limited barrier efficiency against heat and fuel transport. Synergistic improvements in flame retardancy occured for the combinations of AlPi with various nanoparticles with strong condensed-phase activity [16].

PET waste may be suitable in several respects as a raw material for flame retardant insulation foam developments, as it is generated in large quantities due to the increasing use of one-way bottles [17] and it is inherently moderately flammable (V-2 rated acc. UL94 test) due to the presence of heteroatoms in the backbone [18]. It is therefore not surprising that foaming [19–22] and flame retardancy [23–26] of recycled PET are both intensively researched areas. However, at the intersection of the two developments, i.e. in the field of flame retardancy of recycled PET foams, much less successful research has been published. This is because foaming of a low-melt-strength material like PET is rather challenging. The reduced molecular mass of recycled PET can be further degraded by the flame retardants used [27], resulting in inadequate stabilisation during foaming and cell collapse [28]. Depending on the type and amount of flame retardant, the decrease in intrinsic viscosity (IV) can be as high as 0.6–1.0 dL g^{-1} [25, 26], resulting in a significant decrease in melt strength. To compensate degradation, multifunctional chain extenders can be used, which form molecular branches, so that higher porosity can be achieved due to the increased viscosity and melt elasticity [27, 29]. However, producing low-density flame retarded polymer foam is a challenge even from original PET. Another issue is that polymer foams are typically more combustible with the same formulation than bulk (e.g. injection moulded) samples, for two main reasons: the increased contact area between the foamed polymer and air and the reduced volume concentration of the used flame retardants in the expanded foam structures [30, 31].

Bethke et al. [27] produced flame retarded foams with a density of about 0.2 g cm^{-3} starting from PET bottles with IV of 0.76 dL g^{-1} by adding 0.3–0.4 mass% pyromellitic dianhydride (PMDA) type chain extender and 2 mass% phosphonate or mixed phosphonate/phosphate flame retardants with the aid of supercritical CO_2 (sc-CO_2) by extrusion. A 20–30% reduction in peak heat release rate (PHRR) and total heat release (THR) were achieved compared to the non-flame retarded reference, however, foams were not rated by UL94 and Limiting Oxygene Index tests. *Szabó* and *Dogossy* [29] achieved a porosity of 15% by chemical foaming of flame retarded recycled PET raw material. V0 rating was reached using 20% brominated flame retardant.

In previous research studies, the authors achieved positive results regarding PET recycling. On the one hand, V0-rated raw material according to the UL94 standard has been successfully produced from bottle regrind, which also proved to be suitable for the production of injection-moulded electronic components [32]. This was achieved by utilising the synergistic effect of AlPi flame retardant additive (FR) and natural montmorillonite (MMT).

On the other hand, high-porosity foams ($\rho \sim 0.15$ g cm^{-3}) were produced from recycled PET raw material by extrusion foaming with supercritical CO_2 [33]. Adequate viscosity of the starting material was achieved by using a multifunctional epoxide styrene-acrylic oligomer type chain extender besides using 1% talc as the nucleating agent.

The aim of the present research is to develop recycled PET-based foams with improved flame retardant performance, which would significantly broaden the applications of the foams (e.g. construction, automotive, etc.). For this purpose, a suitable composition of the starting material needs to be elaborated. On the one hand, appropriate nucleation is required for cell nucleation [34], on the other hand, adequate viscosity is required for cell growth/stabilisation [35], and also, the ratio of the additives necessary to reduce flammability should be optimised. In this work, composition-property relationships of FR-containing recycled PET foams are comprehensively investigated.

Materials and methods

Materials

rPET bottle flakes (Jász-Plasztik Ltd., Hungary), originating from collected, washed, and sorted post-consumer PET bottles, with an intrinsic viscosity (IV) value of 0.72 ± 0.02 dL g^{-1} were used as matrix material. Joncryl ADR 4468 (BASF, Germany), a multi-functional epoxy-based styrene-acrylic oligomer, was used as chain extender (CE) (specific gravity: 1.08 g cm^{-3}; glass transition temperature: 54 °C). Exolit OP 1240 (Clariant, Muttenzcity, Switzerland) aluminium-tris-(diethylphosphinate) with a phosphorus content of 23.3–24.0% was used as flame retardant (FR)

additive. Cloisite 116 (Byk, Weselcity, Germany) natural montmorillonite (MMT) was used as nanofiller and nucleating agent.

Methods

Sample preparation

Before compounding, the rPET flakes were dried for 4 h at 160 °C. LTE 26-44 (Labtech Engineering, Thailand) twin-screw extruder was used for the mixing with zone temperatures between 245 and 260 °C. The same compounds were used for foaming and injection moulding as well.

Prior to foaming, the regranulates were dried at 160 °C for 4 h. Sc-CO_2-assisted extrusion foaming was carried out on a modified Collin Teach-Line ZK 25 T type co-rotating twin-screw extruder (Dr Collin GmbH, Ebersberg, Germany) with a screw diameter of 25 mm and an L/D ratio of 24. The extruder has five heating zones: 1–3. zone plasticising and melt transport section; CO_2 is introduced into the 4. zone using a syringe pump (Teledyne Isco 260D, Lincoln, NE, USA). This is followed by the last zone 5 of the extruder, followed by the melt pump (T_p) and the static mixer (T_s), which ensure even, homogeneous mixing and material flow. The temperature of these elements and the pressure drop across them were continuously monitored. The die had a circular cross section with an opening of 2 mm in diameter. The continuously exiting foamed products were collected using a conveyor and cooled in the air. During foam extrusion experiments, the screw speed was kept constant at 30 rpm and the following temperature profile was set for the extruder zones: $T_1 = 260$ °C, $T_2 = 270$ °C, $T_3 = 255$ °C and $T_4 = 240$ °C, while T_5, T_p, T_s, and die temperature (T_6) varied during experiments. CO_2 was introduced at a constant volumetric flow rate ranging between 0.5 and 1.5 mL min^{-1}. Once CO_2 was injected, a significant decrease in the material pressure within the extruder barrel occurred, mainly due to the decrease in melt viscosity. Parallel with increasing CO_2 concentration, T_5, T_p, T_s and T_6 were lowered to increase melt strength in the die, typically to 205–220 °C. Once stable conditions were established, samples were collected. The diameter of the manufactured cylindric foamed extrudates varied between 6 and 10 mm, depending on the composition and actual porosity.

For the bulk measurements, 60 mm × 60 mm × 2 mm plaque specimens were injection moulded from the compounded materials using a 50 MEtII (Mitsubishi, Japan) electric injection moulding machine. Zone temperatures varied from 255 to 270 °C, and mould temperature was 60 °C. Injection speed was 75 mm s^{-1}, holding pressure was 40 MPa, and back pressure was 10 MPa. All materials were dried at 160 °C for 4 h before processing.

Characterisation methods

Melt rheology under dynamical shear was investigated using an AR 2000 type rotational rheometer (TA Instruments, New Castle, DE, USA) with 25 mm diameter parallel-plate geometry. Dynamic frequency sweep tests were performed at 260 °C in nitrogen atmosphere to measure the complex shear viscosity over a frequency range of 0.1–100 Hz.

SEM micrographs were obtained using EVO MA 10 instrument (Zeiss, Germany) at an accelerating voltage of 20 kV on specimens coated by 32 nm gold layer. The mean value and standard deviation of the diameter of the cell cross sections approximated by a circle were determined from 50 to 400 measurements per sample. To determine the parameters of cell size distributions, Minitab 17.2.1. statistical software was used.

Void fraction or porosity is defined as a fraction of the volume of voids over the total volume as a percentage. To determine the apparent density, porosity and expansion ratio of the foams, density measurements were performed by immersion method according to ASTM D792-13, using Radwag AS 60/220.R2 analytical balance with density measurement kit in ethanol. The percentage of void fraction (V_f [%]) was calculated from apparent density (ρ_{app}) of foams and the density of the non-foamed extrudate (ρ) according to Eq. (1):

$$V_f = 100\% * \left[1 - \left(\frac{\rho_{app}}{\rho}\right)\right] \tag{1}$$

The crystallisation characteristics of rPET foam samples were determined with a DSC device type DSC131 EVO (Setaram, France). During non-isothermal crystallisation, samples weighting 10–15 mg were heated to 320 °C at a rate of 20 °C min^{-1} and held there for 3 min to erase the thermal prehistory. Subsequent cooling was performed at a rate of 20 °C min^{-1} to − 20 °C. The maximum value of exothermic peaks during cooling was considered to be the crystallisation temperature. The crystallisation enthalpy was measured to calculate the crystallinity of each material according to Eq. (2):

$$CRF = \frac{\Delta h_C}{\Delta h_0 \left(1 - r_{add}\right)} 100\%, \tag{2}$$

where CRF [%] is the crystalline fraction calculated from the crystallisation peak; Δh_C [J g^{-1}] is the measured mass-specific heat flow during the melting (area of the melting peak), Δh_0 [J g^{-1}] is the mass-specific enthalpy of the 100% crystalline PET (140.1 J g^{-1}); r_{add} [–] is the ratio of the used additives.

Thermogravimetric analysis (TGA) measurements were carried out using a TA Instruments Q5000 apparatus (TA Instruments LLC, New Castle, NH, USA) under 25 mL min^{-1} nitrogen gas flow. Samples of about 10 mg

were positioned in open platinum pans. The polymer samples were heated from 25 to 800 °C with a 10 °C min^{-1} rate.

Flammability testing of the foam samples was performed 30 days after production. During this period of time, the foamed extrudates were kept in the open air to ensure gas exchange (from CO_2 to air) in the cells.

Limiting oxygen index (LOI) was determined according to ISO 4589 standard using an apparatus made by Fire Testing Technology Ltd. (East Grinstead, West Sussex, UK). In the case of injection moulded samples, specimens with $100 \times 10 \times 2$ mm^3 dimensions were used, while in the case of foamed materials, cylindrical specimens of 100 mm length were tested.

Standard flammability tests were performed according to UL-94 50W, the specimen dimensions for the injection moulded materials were $100 \times 13 \times 2$ mm^3, while for the foams, cylindrical specimens of 100 mm length were tested.

Comparative mass loss type cone calorimeter (MLC) tests were carried out by an instrument delivered by Fire Testing Technology Ltd. (East Grinstead, West Sussex, UK) according to the ISO 13927 standard method. In the case of injection moulded plates, specimens of 60 mm $\times$ 60 mm $\times$ 2 mm dimensions and 9.9 g nominal mass were tested. In the case of foam samples, 10.0 g of cut cylindrical extudates of 10 mm length were evenly arranged in the alunimium sample holder of 100 mm $\times$ 100 mm size. Both foamed and unfoamed samples were exposed to a constant heat flux of 50 kW m^{-2}. The ignition was provided by a spark plug located 13 mm above the sample. The main characteristics of fire properties, including the maximum of heat release rate (HRR$_{max}$) as a function of time, time-to-ignition (TTI), and total heat release (THR), were determined. When measured at 50 kW m^{-2}, HRR and THR values were reproducible to within $\pm 10\%$.

The mechanical characterisation of the rPET foam samples was carried out by a DMA25 (Metravib, France) type DMA device. Before the test, specimens of 10 mm height were cut, and cross section faces were polished parallel to each other. DMA tests were done in frequency sweep mode at room temperature, in a frequency range 0.01–100 Hz in 6 steps, in compression mode, with ± 20 μm displacement excitation, using 50 μm static displacement. Cross section areas of the specimens were measured by Stemi 508 (Zeiss, Germany) stereomicroscope, and equivalent diameters were calculated to be used as specimen diameters in the measuring program. The storage moduli measured at 1 Hz frequency were analysed and compared in case of all samples. Specific compressive modulus is defined as the ratio between compression storage modulus of the material and its density [36].

Results and discussion

In this work, the flammability of rPET foams was reduced by applying an aluminium-alkylphosphinate type FR additive at 4.0% or 8.0% loading besides using 1.0% MMT that has multiple functions in the system; the nanoclay acts as flame retardant synergist when combined with aluminium-alkylphosphinate [32]; furthermore, it increases melt viscosity and promotes crystallisation as a nucleating agent for adequate foamability [31]. To improve melt rheology, CE was also used at 0.7 or 1.0 mass%. (At CE contents higher than 1.0 mass%, manufacturing difficulties occurred due to high degree of cross-linking and gel generation.)

The composition of the manufactured rPET compounds used in foaming experiments is summarised in Table 1.

The effects of the used additives were comprehensively investigated on the morphology, thermal, flammability and mechanical characteristics of the manufactured rPET foams. For comparison of the thermal and flammability behaviour of bulk and porous rPET materials, injection moulded specimens (rectangular plates) with identical composition were also manufactured and analysed. It has to be noted, however, that the obvious differences in the temperature, residence time and shear conditions of the two processing methods (injection moulding and extrusion foaming) result in PET products with differing degradation state which also affect the properties of the plates and foamed samples.

Investigation of the effects of FR and CE on the rheological properties of rPET

The viscosity curves of rPET compounds used for foaming are presented in Fig. 1. It can be seen that rPET without additives exhibits typical Newtonian behaviour at low frequencies that is associated with its linear molecular structure. Addition of chain extender resulted in viscosity curves typical for pseudoplastic fluids, owing to the disentanglement of the molecular chains with the increase in frequency, in all cases. Incorporation of FR resulted in significant decrease in the complex viscosity due to the reduction in the molecular mass by chain breakage occurred during processing of the

Table 1 Composition of the manufactured rPET compounds

Sample	rPET/%	MMT/%	FR/%	CE/%
0% FR + 0% CE	99.0	1.0	0.0	0.0
0% FR + 0.7% CE	98.3	1.0	0.0	0.7
4% FR + 0.7% CE	94.3	1.0	4.0	0.7
4% FR + 1.0% CE	94.0	1.0	4.0	1.0
8% FR + 0.7% CE	90.3	1.0	8.0	0.7
8% FR + 1.0% CE	90.0	1.0	8.0	1.0
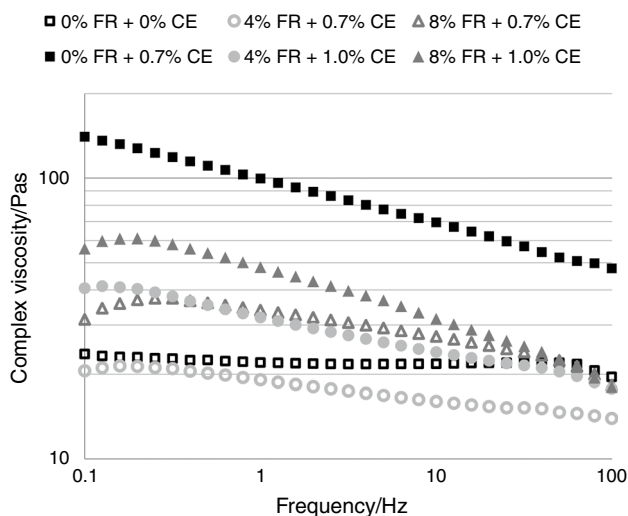
Fig. 1 Melt viscosity of the rPET compounds used for foaming

Fig. 2 Porosity of foams as a function of FR content and CE ratio

flame retardant containing compounds. Nevertheless, the compound with the higher (8%) FR content exhibits higher complex viscosity, which is likely due to the increased physical hindrance between the filler and the polymer that reduces flowability. Also, by adding more FR additive, the number of reactive sites in the polymer chains may also increase. The complex viscosity of the FR containing compounds noticeably increased when the amount of CE was increased from 0.7 to 1.0%, and parallelly, shear-thinning became more pronounced which indicates increased number of long-chain branches in these systems. It is supposed that the same dosage of CE in the flame retarded rPET systems (with shorter molecular chains) results in higher cross-link density than in FR additive-free rPET. Up to a certain degree, increased cross-link density is favourable in terms of cell stabilisation during foaming, however, too high cross-link density can restrict expansion.

Morphological characterisation of the foams

During processing of each rPET compound, samples were collected after stable conditions were reached for continuous manufacturing of low-density foams. The typical porosity ranges obtained as a function of FR ratio and CE content are plotted in Fig. 2. It can be seen that without CE, the melt strength of rPET is insufficient to create a foam structure with very high porosity (i.e. $V_f > 80\%$). As a result of 0.7% CE addition, however, porosity as high as 90% was achieved from rPET. Similar result was obtained in our earlier study when talc was used as nucleating agent besides 0.7% CE in bottle grade rPET [33]. The achievable porosity range decreased with increasing FR content, likely due to the reducing chain length and increasing stiffness of the polymer matrix. Also, the limited polymer-filler interaction
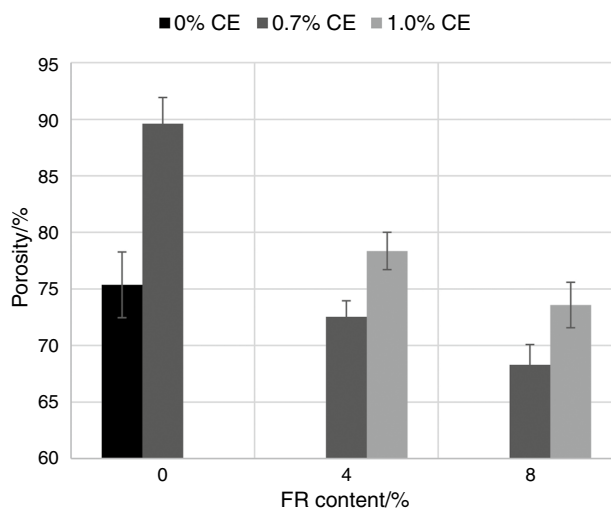
may cause an increased number of interfacial defects, which favour the escape of CO_2, thus hindering the expansion. Increasing the ratio of CE from 0.7 to 1.0% slightly compensated the former effects; as a result of increased cross-link density (see Fig. 1), the cell stabilisation became more effective, and thus, noticeably, higher porosity values were reached. At 8% FR content, porosity higher than 70% proved to be still achievable. Considering the porosity results, further increase in the CE content may be favourable, however, at CE ratio higher than 1.0 mass%, manufacturing difficulties occur due to significant gel generation.

The cellular structure of the rPET foams of six different compositions was further analysed. SEM images taken from the cross sections of the rPET foams are shown in Fig. 3, while the corresponding cell-size distributions determined based on SEM image analyses are presented in Fig. 4. The cell diameter distribution characteristic for the FR-free foams is not plotted in Fig. 4, since the cross section of these foam samples contains only a few number but large cells (with diameters even higher than 1 mm). The density function of the normal distribution was fitted to the measurement points with a class width of 50 microns. Normal probability density function **Eq. (3) was fitted to the measuring points; the corresponding median and standard deviation parameters as a function of FR content are shown in Fig. 5.

$$f_{nd}(d) = \frac{1}{\sigma\sqrt{2\pi}} \cdot e^{-\frac{(d-m)^2}{2\sigma^2}}, \qquad (3)$$

where $f_{nd}(d)$ is the normal probability density function of the cell diameters; σ is the standard deviation, and m is the mean value of the cell diameters (d).

Based on the SEM images, no indication was found that the increasing open cell ratio would cause the decreasing

Fig. 3 SEM images images taken from the cross section of foam samples: **a** 0% CE + 0% FR; **b** 0.7 CE + 0% FR; **c** 0.7% CE + 4% FR; **d** 1.0% CE + 4% FR; **e** 0.7% CE + 8% FR; **f** 1.0 CE + 8% FR
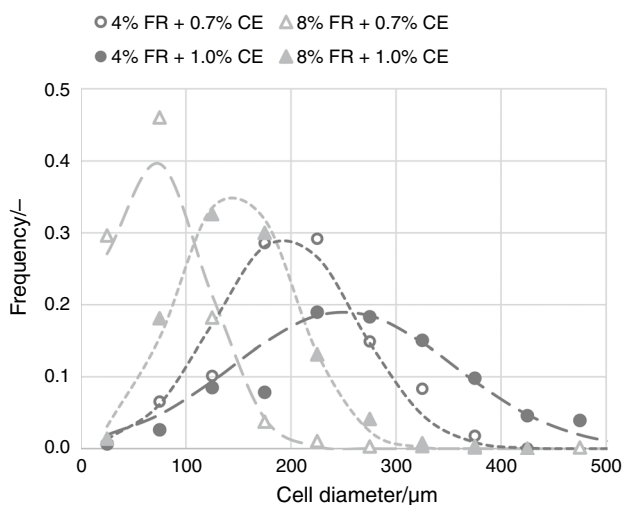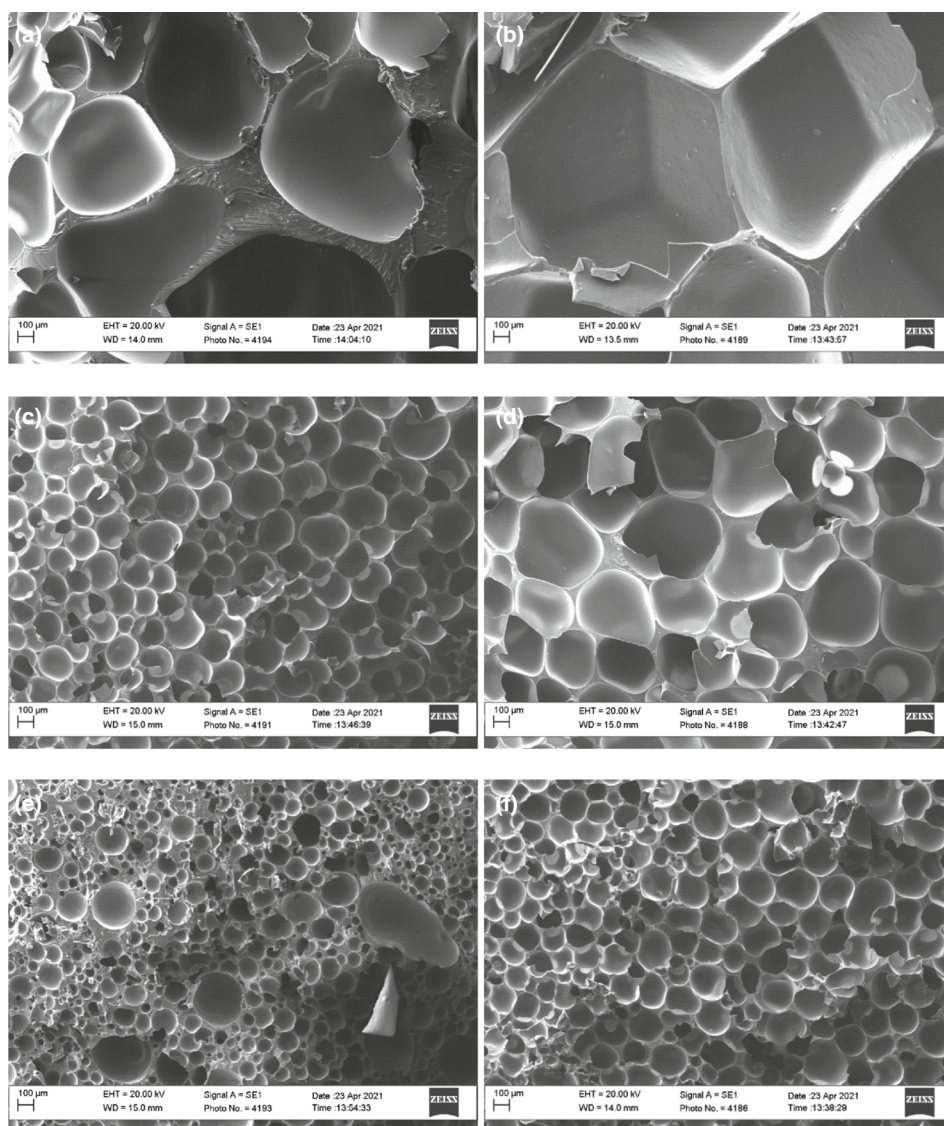

Fig. 4 Distributions of cell diameters in different foam samples

void fraction as a function of FR content. More likely explanation is the insufficient strength and elasticity of the FR-containing polymer melt. It is visible that the average cell diameter decreases with increasing FR content, also indicating that the cell walls composed of shorter and less elastic molecular chains are less capable of expanding. The cellular structure of the 8% FR + 0.7% CE containing foam sample was found to be less uniform, likely as a result of cell coalescence due to weak melt strength. At the same time, the average cell diameter of the FR-containing foams slightly increased when a higher amount (1.0%) of CE was used. The cross-links introduced by the CE may compensate the harmful effect of the reduced chain length of the FR containing rPET and increase melt elasticity. As a consequence, cells are less prone to collapse during growth. The improved expansion ability is also reflected by the higher porosity ranges reached for these materials (Fig. 2).

Fig. 5 Parameters of density functions of cell diameter distributions
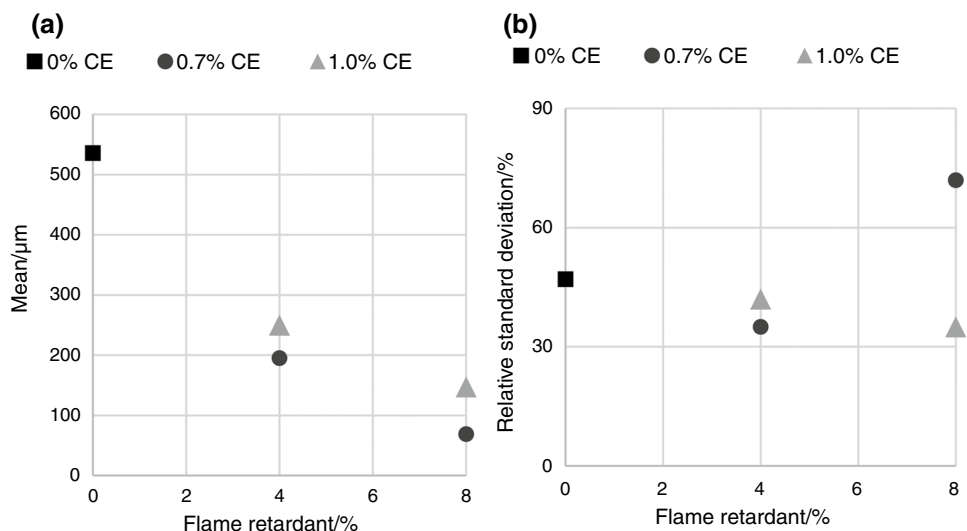
The crystallisation ability of polymers is strongly related to their structure [37]. DSC measurements were performed on the FR-containing rPET foams to indirectly analyse the structural changes in the polymer chains that occurred during processing. Crystallisation results derived from the cooling cycle are shown in Fig. 6. The resulting effect of two factors can be seen. On the one hand, the ability for crystal formation increases with increasing FR content that is associated with the decreasing molecular chain length. On the other hand, use of CE hinders crystallisation due to decreased macromolecular regularity and reduced mobility of the cross-linked rPET chains. As a result, the crystallisation temperature of the FR-containing rPET foams decreases when the CE ratio is increased to 1.0%, therefore, highly branched but short molecular chains are proposed for these materials. This assumption is in agreement with the rheological behaviour (Fig. 1) and expansion ability (Fig. 2) of these compounds.

Thermal and flammability characteristics

The thermal behaviour of the rPET compounds before and after foaming was analysed using TGA. In Fig. 7, the initial decomposition temperature (determined at 5% mass loss) and the residual mass obtained at 500 °C are compared, respectively. It is visible that with the increase in FR content, the initial degradation temperature decreases, but in parallel, the degree of carbonisation increases resulting in a noticeable amount (21–24%) of char that is essential for effective flame retardant performance. The foam samples start to decompose at slightly lower temperature than the corresponding bulk materials which is due to the reduced molecular mass of the extrusion foamed materials (and is not associated with the porous structure). Nevertheless, there is no noticeable difference in terms of residual mass, i.e. the foams can char as well as the bulk materials under the conditions of a TGA analysis. Based on this, homogeneous

Fig. 6 Crystallisation characteristics derived from cooling cycle of DSC analyses
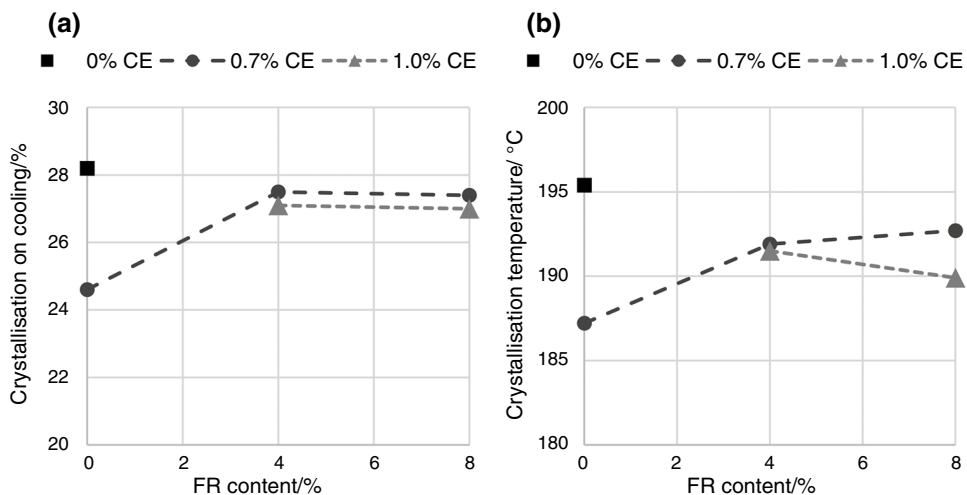
Fig. 7 **a** Decomposition temperature and **b** residual mass derived from TGA analyses
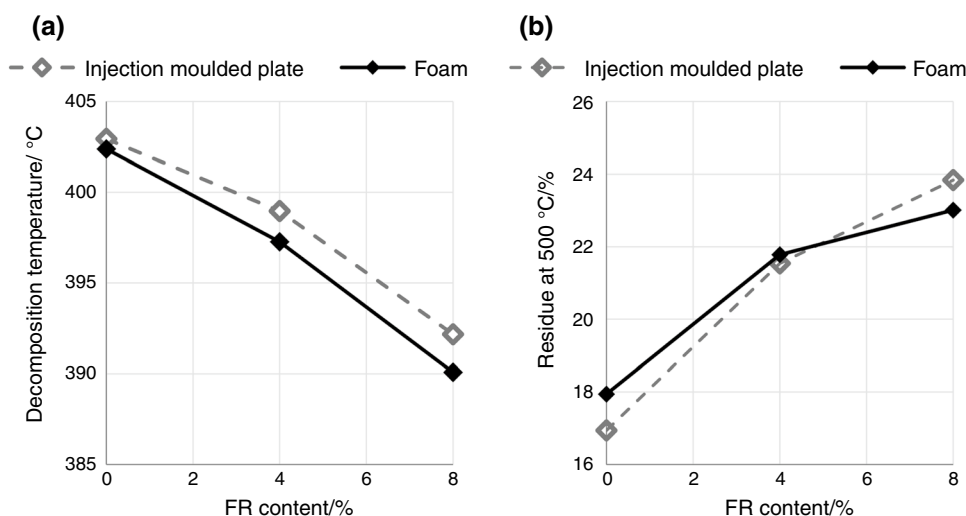

Table 2 UL94 ratings of rPET foams and injection moulded plates (n.d.: no data)

	FR content/%						
		0		4		8	
		Foam	Plate	Foam	Plate	Foam	Plate
CE content [%]	0.0	V2	V2	n.d	V0	n.d	V0
	0.7	V2	V2	V2	V2	V0	V0
	1.0	n.d	n.d	V2	V2	V0	V0

distribution of the additives within the cellular structure can be suggested.

Flammability of the FR-containing rPET foams and injection moulded plates was characterised according to the UL94 standard. The obtained UL94 ratings are summarised in Table 2. In the case of injection moulded samples, in accordance with our previous results [32], combination of 4% FR with 1% MMT sufficed to reach V0 classification. Self-extinguishing behaviour is observed as the FR containing melted polymer falls away from the flame front, taking away the heat and flaming material from the ignition source. The use of CE besides the same FR system, however, inhibits this "melt-away" effect [38–40], and thus, the UL94 rating falls back to V2. At 8% FR ratio besides 1% MMT, V0 rating proved to be achievable independently from the CE concentration and the porosity (bulk or foamed) of the tested sample.

Nevertheless, the highly porous foams proved to be noticeably more flammable during LOI measurements than the bulk counterparts. As presented in Fig. 8, at identical FR content, 2–3% lower LOI values were measured for the foams compared to the bulk samples. The reduction in LOI after foaming is mainly attributed to the increased contact area between the rPET matrix and air and also to the decreased volume concentration of the used flame retardants in the expanded foam structures [30, 31, 41]. Still, at
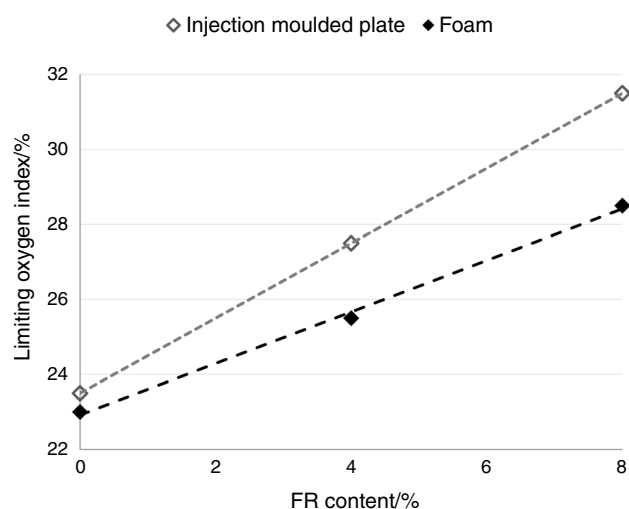

Fig. 8 LOI values of rPET foams and injection moulded plates

higher FR concentration, i.e. with 8% FR and 1% MMT, a LOI value as high as 28.5% was reached in rPET foams of 70% porosity.

Comparative mass loss type cone calorimeter tests were performed to investigate the combustion behaviour of the flame retarded rPET foams and injection moulded plates with 1% CE content.

The gained Heat Release Rate (HRR) curves are presented in Fig. 9, while numerical test results are summarised in Table 3. From the collected data, Flame Retardancy Index (FRI) of the flame retarded foams and plate samples was calculated according to the formula of *Vahabi* and *Saeb* [42] by considering the corresponding FR-free foam and plate sample as reference, respectively. It can be seen in Fig. 9a that with the increase in FR ratio, the fire retardant performance of the rPET foams improved noticeably. About 32% reduction in HRR_{max} was measured with 4% FR + 1% MMT content, which is comparable with the results of *Altstädt* et al., who reported a 29% reduction in HRR_{max} by the addition of 5% zinc diethyl phosphinate (DEPZn) in foamed bottle-grade PET [27]. By increasing the FR ratio, the fire retardant performance further improved; TTI increased up to 45 s, HRR_{max} reduced by 49%, time of HRR_{max} further shifted in time, and THR reduced by 30%. The shape of the HRR curves corresponding to the foam samples indicates limited charring but strong gas-phase activity [43]. The observed significant increase in TTI and reduced HRR_{max} and THR values are mainly due to efficient flame inhibition of the used FR, while the char promoting activity of MMT is less pronounced in the case of the foams. The FRI of the rPET foams increased to 2.0 and 3.9 with 4 and 8% FR, respectively,

meaning "good" fire retardancy performance [42]. Nevertheless, since flame inhibition is the dominant mode of action of the used FR, which leads to incomplete combustion, increase in total smoke release and CO yield is expected during combustion of these flame retarded materials. This assumption is also supported by the experimental results of *Schartel* et al. obtained from PBT/AlPi systems [15, 16].

The cone calorimetry results of the injection moulded plates are presented in Fig. 9b and Table 3, respectively. The more widened shape of the HRR curves indicates more efficient condensed-phase activity of the used FR system in the bulk materials than in the case of the foam samples. In accordance to this, it can also be observed that the same amount of FR reduced the THR of bulk samples somewhat more effectively than that of foams. This also supports our finding that, when exposed to high heat flux, the char promoting efficiency of the used mineral clays is very limited in highly porous foams, compared to bulk materials. In contrast, the applied FRs proved to be more effective in increasing the TTI and reducing the HRR_{max} of the foamed samples compared to the bulk counterparts. *Altstädt* et al. also observed that the foamed PET samples require somewhat less amount of FR than corresponding bulk samples for a quantifiable fire retardant efficiency

Fig. 9 Results of the cone calorimeter tests (**a**: foam samples; **b**: plate samples)
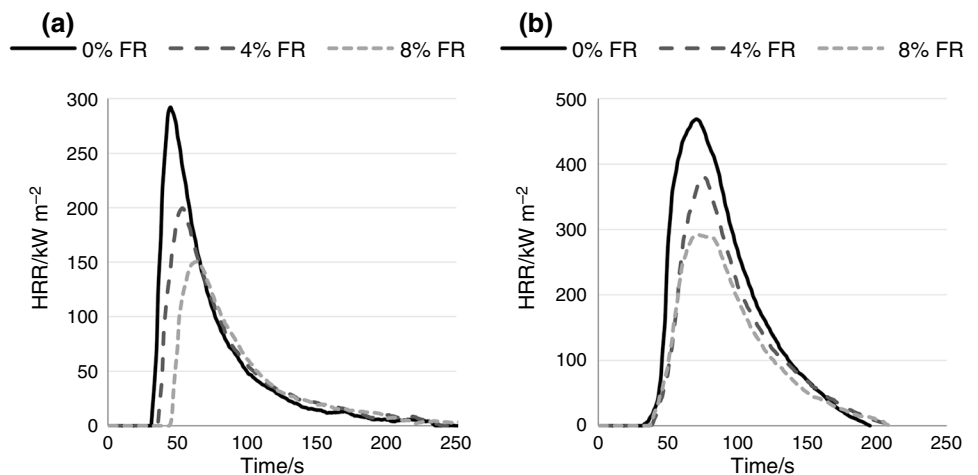

Table 3 Numerical results of cone calorimeter tests

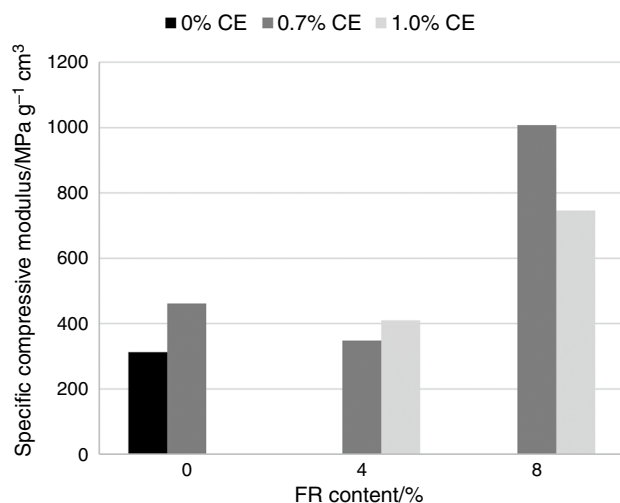| FR content/%	TTI/s	HRR_{max}/kWm^{-2}	HRR_{max} reduction/%	HRR_{max} time/s	THR/MJm^{-2}	THR reduction/%	FRI/–
Foam samples							
0	32	292	–	45	12.1	–	1.0
4	36	199	32	53	10.2	16	2.0
8	45	150	49	64	8.5	30	3.9
Plate samples							
0	33	468	–	71	29.6	–	1.0
4	37	381	19	75	22.8	23	1.8
8	34	292	38	72	19.6	34	2.5

Fig. 10 Specific compressive modulus of the foams as determined by DMA at 1 Hz

[27]. This phenomenon is related to the thermal insulating properties of the porous foams.

Mechanical properties

The mechanical performance of the flame retarded rPET foams was characterised using a DMA device. Storage moduli of the foams with six different compositions were determined at 1 Hz at room temperature. Then, the density-related modulus, as specific property, was used for comparison of the mechanical performance of the foam samples. It can be seen in Fig. 10. that the lower FR ratio (4%) does not noticeably affect the specific compressive modulus of the foams, while at 8% FR content, the stiffening effect of the additive already occurs. The more than twofold increase in the specific compressive modulus of the 8% FR containing foams is, however, also associated with their smaller average cell size (see Fig. 5a). Increasing the amount of CE from 0.7 to 1.0% resulted in increase in the average cell diameter of the FR-containing foams, and parallelly, their (non-specific) compressive modulus decreased. The density-related specific modulus of the 4% FR containing foam remained almost unchanged when the CE content was increased to 1.0%, likely as a result of opposing effects of porosity increase and cell size decrease.

Conclusions

In this study, the synergistic combination of FR and MMT was utilised to provide flame retardancy to rPET foams, manufactured by sc-CO_2-assisted extrusion. Besides the FR additives, 0.7 or 1.0% of CE was applied in all cases.

It was found that increasing FR concentration causes a significant decrease in the chain-length of the rPET molecules during processing, thereby reducing the viscosity and strength of the polymer melt, while reducing the average cell diameter and achievable porosity range of the flame retarded foams. Adding 1.0% CE besides the FR improves melt strength of rPET by extensive cross-linking of fragmented chains so that higher rates of expansion become achievable. At 8% FR concentration, foams with porosity higher than 70% accompanied with uniform cellular structure were produced which have prominent flame retardant characteristics: pass V0 classification, according to the UL94 standard, has a LOI of 28.5%, and by 50% reduced peak of heat release rate and by 30% reduced total heat emission during cone calorimeter tests comparing to the additive-free counterpart.

When compared to bulk materials of identical composition, it was concluded that the increased amount of CE necessitated in foams inhibits the flame extinguishing "melt-away" effect so that a fire can spread by flaming drops. Also, the increased contact area between the rPET matrix and air in the highly porous foam samples results in increased flammability. As a consequence, higher amount of FR is needed to reach V0 classification or the same LOI value in foams than in bulk materials. The used AlPi type FR additive, known to be mainly active in the gas phase [15], proved to be especially effective in increasing TTI, and reducing HRR_{max} and THR during combustion of the foams. Nevertheless, the char promoting effect of MMT was found to be less pronounced in porous materials than in bulk samples.

Considering the mechanical properties of the flame retarded rPET foams, 4% FR does not noticeably affect the performance, while higher loading of the additives (8% FR) was found to significantly increase the stiffness, characterised by the density-related compressive modulus.

Flame retarded foam products prepared from secondary raw materials may find applications in the construction or transportation industry as lightweight heat insulator or sandwich core materials.

References

1. (USFA) United States Fire Administration. Residential Building Fires (2017 – 2019). 2011;12:1–17.
2. Delva L, Hubo S, Cardon L, Ragaert K. On the role of flame retardants in mechanical recycling of solid plastic waste. Waste Manag. 2018;82:198–206.
3. Çalışkan E, Çanak TÇ, Karahasanoğlu M, Serhatlı IE. Synthesis and characterization of phosphorus-based flame retardant containing rigid polyurethane foam. J Therm Anal Calorim. 2021
4. Kodur V, Kumar P, Rafi MM. Fire hazard in buildings: review, assessment and strategies for improving fire safety. PSU Res Rev. 2019;4:1–23.
5. Samani P, van der Meer Y. Life cycle assessment (LCA) studies on flame retardants: A systematic review. J Clean Prod. 2020;274:123259.
6. Schyns ZOG, Shaver MP. Mechanical recycling of packaging plastics: a review. Macromol Rapid Commun. 2021;42:1–27.
7. Shuangjun C, Weihe S, Haidong C, Hao Z, Zhenwei Z, Chaonan F. Glycolysis of poly(ethylene terephthalate) waste catalyzed by mixed Lewis acidic ionic liquids. J Therm Anal Calorim. 2021;143:3489–97.
8. Geyer R, Jambeck JR, Law KL. Production, use, and fate of all plastics ever made. Sci Adv. 2017;3:25–9.
9. Gubanova E, Kupinets L, Deforzh H, Koval V, Gaska K. Recycling of polymer waste in the context of developing circular economy. Archit Civ Eng Environ. 2020;12:99–108.
10. Sardon H, Dove AP. Plastics recycling with a difference. Science. 1979;2018(360):380–1.
11. Banhegyi Gy. Reconsidering plastics recycling and bio-plastics. Express Polym Lett. 2021;15:685–6.
12. Foschi E, Bonoli A. The Commitment of packaging industry in the framework of the european strategy for plastics in a circular economy. Adm Sci. 2019;9:18.
13. Morgan AB. The future of flame retardant polymers-unmet needs and likely new approaches. Polym Rev. 2019;59:25–54.
14. Rakotomalala M, Wagner S, Döring M. Recent developments in halogen free flame retardants for epoxy resins for electrical and electronic applications. Materials. 2010;3:4300–27.
15. Braun U, Schartel B. Flame retardancy mechanisms of aluminium phosphinate in combination with melamine cyanurate in glass-fibre-reinforced poly(1,4-butylene terephthalate). Macromol Mater Eng. 2008;293:206–17.
16. Brehme S, Köppl T, Schartel B, Altstädt V. Competition in aluminium phosphinate-based halogen-free flame retardancy of poly(butylene terephthalate) and its glass-fibre composites. E-Polymers. 2014;14:193–208.
17. Wang Y, Gu Y, Wu Y, Zhou G, Wang H, Han H, et al. Performance simulation and policy optimization of waste polyethylene terephthalate bottle recycling system in China. Resour Conserv Recycl. 2020;162: 105014.
18. Shi J, Zeng W, Yang Z, Li J, Zhao P, Li H, et al. Effect of particle size on flame retardancy and mechanical properties of hydroxyethyl diphosphate modified aluminum hydroxide intrinsic polyethylene terephthalate. J Appl Polym Sci. 2021;138:50500.
19. Cadete MS, Gomes TE, Carvalho PJ, Neto VF. Polymeric foams from recycled thermoplastic poly(ethylene terephthalate). J Cell Plast. 2020;0021955X2094856.
20. Szabó VA, Dogossy G. Structure and properties of closed-cell foam prepared from rPET. IOP Conf Ser Mater Sci Eng. 2018;426: 012043.
21. Bocz K, Molnár B, Marosi G, Ronkay F. Preparation of low-density microcellular foams from recycled PET modified by solid state polymerization and chain extension. J Polym Environ. 2019;27:343–51.
22. Coccorullo I, Di ML, Montesano S, Incarnato L. Theoretical and experimental study of foaming process with chain extended recycled PET. Express Polym Lett. 2009;3:84–96.
23. Marques DV, Barcelos RL, Parma GOC, Girotto E, Júnior AC, Pereira NC, et al. Recycled polyethylene terephthalate and aluminum anodizing sludge-based boards with flame resistance. Waste Manag. 2019;92:1–14.
24. Thumsorn S, Negoro T, Thodsaratpreeyakul W, Inoya H, Okoshi M, Hamada H. Effect of ammonium polyphosphate and fillers on flame retardant and mechanical properties of recycled PET injection molded. Polym Adv Technol. 2017;28:979–85.
25. Gooneie A, Simonetti P, Salmeia KA, Gaan S, Hufenus R, Heuberger MP. Enhanced PET processing with organophosphorus additive: Flame retardant products with added-value for recycling. Polym Degrad Stab. 2019;160:218–28.
26. Chen L, Ni Y, Fu T, Wang Y, Liu B, Wang X. New methods for flame-retarding PET without melt dripping. Chin Sci Bull. 2020;65:3160–72.
27. Bethke C, Goedderz D, Weber L, Standau T, Döring M, Altstädt V. Improving the flame-retardant property of bottle-grade PET foam made by reactive foam extrusion. J Appl Polym Sci. 2020;137:49042. https://doi.org/10.1002/app.49042.
28. Szabó VA, Dogossy G. Flame retardancy of recycled PET foam. IOP Conf Ser Mater Sci Eng. 2020;903: 012048.
29. Szabó VA, Dogossy G. Investigation of flame retardant rPET foam. Periodica Polytech Mech Eng. 2019;64:81–7.
30. Wang J, Ren Q, Zheng W, Zhai W. Improved flame-retardant properties of Poly(lactic acid) foams using starch as a natural charring agent. Ind Eng Chem Res. 2014;53:1422–30. https://doi.org/10.1021/ie403041h.
31. Vadas D, Igricz T, Sarazin J, Bourbigot S, Marosi G, Bocz K. Flame retardancy of microcellular poly(lactic-acid) foams prepared by supercritical CO2-assisted extrusion. Polym Degrad Stab. 2018;153:100–8.
32. Ronkay F, Molnár B, Szalay F, Nagy D, Bodzay B, Sajó IE, et al. Development of flame-retarded nanocomposites from recycled PET bottles for the electronics industry. Polymers (Basel). 2019
33. Bocz K, Ronkay F, Molnár B, Vadas D, Gyürkés M, Gere D, et al. Recycled PET foaming: supercritical carbon dioxide assisted extrusion with real-time quality monitoring. Adv Ind Eng Polym Res. 2021; Available from: https://linkinghub.elsevier.com/retrieve/pii/S2542504821000154
34. Chauvet M, Sauceau M, Fages J. Extrusion assisted by supercritical CO 2 : a review on its application to biopolymers. J Supercrit Fluids. 2017;120

35. Villamil Jiménez JA, le Moigne N, Bénézet J-C, Sauceau M, Sescousse R, Fages J. Foaming of PLA composites by supercritical fluid-assisted processes: a review. Molecules. 2020;25

36. Zúñiga C, Lligadas G, Ronda JC, Galià M, Cádiz V. Self-foaming diphenolic acid benzoxazine. Polymer (Guildf). 2012;53:3089–95.

37. Ronkay F, Molnár B, Nagy D, Szarka G, Iván B, Kristály F, et al. Melting temperature versus crystallinity: new way for identification and analysis of multiple endotherms of poly(ethylene terephthalate). J Polym Res. 2020;27:372. https://doi.org/10.1007/s10965-020-02327-7.

38. Tao W, Li J. Melamine cyanurate tailored by base and its multi effects on flame retardancy of polyamide 6. Appl Surf Sci. 2018;456

39. Sun J, Li L, Li J. Effects of furan-phosphamide derivative on flame retardancy and crystallization behaviors of poly(lactic acid). Chem Eng J. 2019;369

40. Horrocks AR, Nazaré S, Kandola B. The particular flammability hazards of nightwear. Fire Saf J. 2004;39:259–76.

41. Wang K, Wang J, Zhao D, Zhai W. Preparation of microcellular poly(lactic acid) composites foams with improved flame retardancy. J Cell Plast. 2017;53

42. Vahabi H, Kandola B, Saeb M. Flame retardancy index for thermoplastic composites. Polymers (Basel). 2019;11

43. Schartel B, Hull TR. Development of fire-retarded materials—Interpretation of cone calorimeter data. Fire Mater. 2007;31:327–54.